

Secondary positrons and electrons measured by PAMELA experiment

V.V. Mikhailov¹, O. Adriani⁷, G. Barbarino², G.A. Bazilevskaya³, R. Bellotti⁴, M. Boezio⁵, E.A. Bogomolov⁶, M. Bongi⁷, V. Bonvicini⁵, S. Bottai⁷, A. Bruno⁴, F.S. Cafagna⁴, D. Campana², P. Carlson⁸, M. Casolino⁹, G. Castellini¹⁰, C. De Donato⁹, C. De Santis⁹, N. De Simone⁹, V. Di Felice⁹, A.M. Galper¹, A.V. Karelin¹, S. V. Koldashov¹, S. Koldobsky¹, S.Yu. Krutkov⁶, A.N. Kvashnin³, A. A. Leonov^{1,3}, V.V. Malakhov¹, Yu.V. Mikhailova¹, L. Marcelli⁹, M. Martucci^{9,12}, A.G. Mayorov¹, W. Menn¹¹, M. Merge^{9,13}, E. Mocchiutti⁵, A. Monaco⁴, N. Mori¹⁰, R. Munini⁵, G. Osteria², P. Papini⁷, F. Palma^{9,13}, B. Panico², M. Pearce⁸, P. Picozza^{9,13}, M. Ricci¹², S.B. Ricciarini⁷, M. F. Runtso¹, M. Simon¹¹, R. Sparvoli^{9,13}, P. Spillantini¹, Yu. I. Stozhkov³, A. Vacchi⁵, E. Vannuccini⁷, G.I. Vasiliev⁶, S.A. Voronov¹, Yu. T. Yurkin¹, G. Zampa⁵, N. Zampa⁵

¹ *National Research Nuclear University MEPhI (Moscow Engineering Physics Institute), Kashirskoe highway 31, Moscow, 115409, Russia*

² *INFN, Sezione di Naples and Physics Department of University of Naples Federico II*

³ *Lebedev Physical Institute, Russia*

⁴ *INFN, Sezione di Bari Physics and Department of University of Bari, Italy*

⁵ *INFN, Sezione di Trieste, Italy*

⁶ *Ioffe Physical Technical Institute, Russia*

⁷ *INFN, Sezione di Florence and Physics Department of University of Florence, Italy*

⁸ *KTH, Department of Physics,*

and The Oskar Klein Centre for Cosmoparticle Physics, Sweden

⁹ *INFN, Sezione di Rome "Tor Vergata", Italy*

¹⁰ *INFN, IFAC, Italy*

¹¹ *Universität Siegen,*

Department of Physics, Siegen, Germany

¹² *INFN, Laboratori Nazionali di Frascati, Italy*

¹³ *University of Rome Tor Vergata,*

Department of Physics, Italy

¹⁴ *Agenzia Spaziale Italiana (ASI) Science Data Center, Frascati, Italy*

We present a measurements of electron and positron fluxes below the geomagnetic cutoff rigidity in wide energy range from 50 MeV to several GeV by the PAMELA magnetic spectrometer. The instrument was launched on June 15th 2006 on-board the Resurs-DK satellite on low orbit with 70 degrees inclination and altitude between 350 and 600 km. The procedure of trajectories calculations in the geomagnetic field separates stably trapped and albedo components produced in interactions of cosmic ray protons with the residual atmosphere from galactic cosmic rays. Features of spatial distributions of secondary electrons and positrons in the near Earth space, including the South Atlantic Anomaly, were investigated.

High energy primary cosmic rays produce secondary particles in nuclear interactions in atmosphere. A part of charged secondaries produced at the top of atmosphere can travel backward in space along the Earth's magnetic field lines. Flux of secondary electrons with energy $E > 100$ MeV was first calculated in paper [1]. In this work it was considered process of charged pions decay produced in cosmic ray proton interactions. Pions decay throw $\pi^\pm \rightarrow \mu^\pm \rightarrow e^\pm$ chain to electrons and positrons. Because production rate is proportional to cosmic ray intensity I_{cr} , residual atmosphere density $\rho(h)$ and particle's time of live T is $\propto 1/\rho(h)$ then resulting intensity of secondary particles $J(h) \propto I_{cr} \cdot \rho \cdot T$ will be approximately constant with altitude in wide range forming some kind of a halo around the Earth. Nuclear interactions of trapped protons of energies > 300 MeV with upper atmosphere constituents could be considered for the production of positrons and electrons via the same pion decay process in the innermost magnetosphere. Calculations performed in paper [2] predict the existence of a sec-

ondary belt in a narrow region around L-shell = 1.2. The flux ratio of positrons to electrons e^+/e^- is estimated to be ~ 4 for energies of 40-1500 MeV. This mechanism exhibits sharply decreasing spectrum with energy. At 200-300 MeV energies, positron fluxes from the trapped proton source are still comparable with the cosmic ray born positrons, but at higher energies production by trapped protons is negligible.

The magnetic spectrometer PAMELA was launched onboard the Resurs-DK1 satellite on the 15th of June 2006. The satellite had a quasi-polar (70° inclination) elliptical orbit at an altitudes between 350 and 600 km. Preliminary results of PAMELA observation of secondary electron and positron fluxes near the Earth made in first year of the flight were reported in paper [3]. The backtracing procedure which determines tracks of particles before their detection offers new opportunities to compare data with models and it allows to determine individual particles origin [4, 5]. This work presents PAMELA spectrometer measurements of spatial distributions of secondaries electrons and

positrons made using trajectory analysis.

I. PAMELA SPECTROMETER

The instrument consists of a Time-of-Flight system (TOF), an anticoincidence system, a magnetic spectrometer, an electromagnetic calorimeter, a shower tail catching scintillator and a neutron detector. The TOF system provides the main trigger for particle acquisition, measures the absolute value of the particle charge and its flight time while crossing the apparatus (the resolution is better than 350 psec). A rigidity is determined by the magnetic spectrometer, composed by a permanent magnet with a magnetic field intensity 0.4 T and a set of six double-side micro-strip silicon detectors. The electron and positron identification is provided by the imaging calorimeter which consist of a series of 44 strip silicon layers interleaved by 22 tungsten planes (16.3 radiation and 0.6 nuclear interaction lengths deep). Particles not cleanly entering the PAMELA acceptance are rejected by the anticoincidence system. Using of the TOF system, the magnetic spectrometer and additional analysis of the calorimeter information allows extracting electrons and positrons and measuring their energy (from 50 MeV to several hundred GeV) effectively. The acceptance of the instrument is about $21.6 \text{ cm}^2\text{sr}$ [6].

II. DATA ANALYSIS

For each registered event the following parameters were measured or calculated: the number of tracks; averaged energy losses in the magnetic spectrometer planes; the rigidity and the track length (by fitting the track in the magnetic field); the time of flight. A particle velocity was calculated using the time of flight and the track length. Moreover, a set of variables dealing with point of interaction, transversal and longitudinal profiles was calculated using the calorimeter data [6].

Electrons and positrons were identified using information about dE/dx energy losses in the spectrometer planes to determine charge $Z=1$, shower properties in the electromagnetic calorimeter, particle velocity and a rigidity. The misidentification of protons and pions is the largest source of background. Particle identification based on the calorimeter data can be tuned to rejection power $10^4 - 10^5$ for protons and pions, while selecting $> 80\text{-}90\%$ of the electrons or positrons over all energy range.

Total accumulated statistic for electrons and positron is about 4×10^6 in whole energy range.

Gathering power of the instrument was estimated with Monte-Carlo simulation with official PAMELA Collaboration software [6]. An efficiency of the instrument may change with time and must be taken into

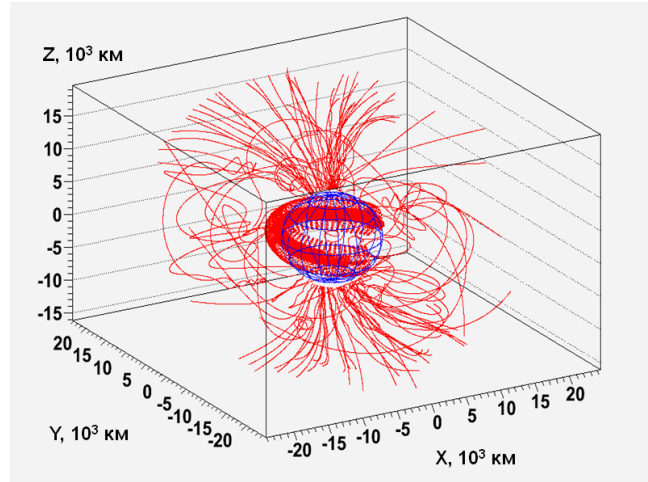


FIG. 1: Examples calculated trajectories of electrons and positrons detected during several orbits

account carefully in a data proceeding. It was verified from experimental data itself by using different combination of information from imaging calorimeter, magnetic spectrometer and time of flight system.

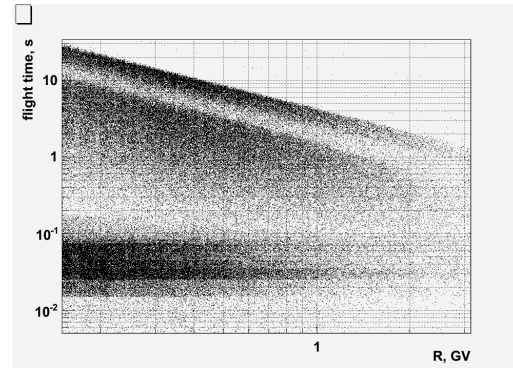


FIG. 2: Flight time vs particle's rigidity.

Using a geographical coordinates and an orientation of PAMELA as a function of time, the McIlwain geomagnetic coordinates L-shell and B were calculated for every event. For the calculation, the IGRF model (<http://nssdcftp.gsfc.nasa.gov/models/geomagnetic/igrf>) of the Earth magnetic field was used.

The main axis of PAMELA points to a local zenith. Orbit characteristics allow measuring particles with pitch angles (the angle between the particle velocity and the magnetic field vector) of about $80\text{-}90^\circ$ in the equatorial region.

Primary particles are observed mainly in polar regions and above cut-off rigidity near equator. This component consist of mainly electrons. Secondary component with small pitch-angles is observed below geomagnetic cut-off for all latitudes and secondary trapped particles can be measured in South Atlantic Anomaly (SAA) with pitch-angles about 90°

[3, 7].

To determine primary or secondary origin of detected particles the backtracing procedure was applied for every identified events to obtain trajectory of events up to 35 second before detection. The tracing was stopped if particles touched the Earth atmosphere on 40 km altitude or escaped magnetosphere. Escaping boundary was chosen to be 20000 km. Trajectory allows to determine particle origin for every individual event. Figure 1 shows examples calculated trajectories of electrons and positrons detected during several orbits. Totally about 10^6 events were back-traced. Finally, primary electrons and positrons with high rigidity R were excluded from analysis together with particles in transition region near geomagnetic cut-off, applying condition $R < 10/L^3$ [GV], where L is geomagnetic L-shell.

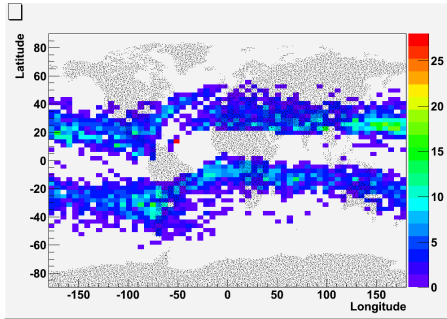


FIG. 3: Regions where short-lived positrons were originated.

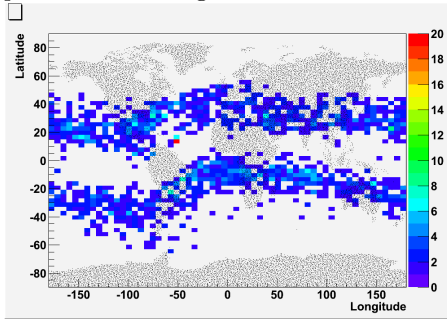


FIG. 4: Regions where short-lived electrons were originated.

III. RESULTS

Calculations of particle trajectories in geomagnetic field provides additional information about spatial distribution of secondary fluxes in the Earth vicinity because it gives possibility to explore fluxes in enlarged regions outside the satellite orbits. In figure 2 time of flight in magnetosphere versus of rigidity in magnetosphere is shown for equatorial region ($L < 2$). Typically reentrant albedo particles reach the orbit of the

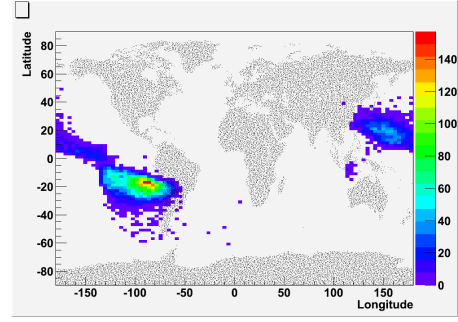


FIG. 5: Regions where quasi-trapped positrons were originated.

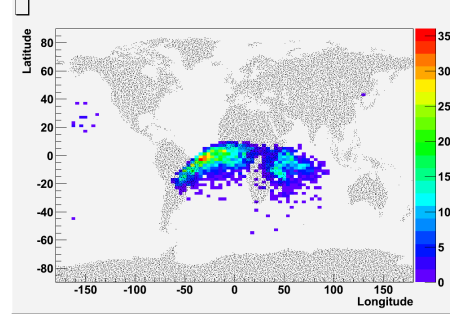


FIG. 6: Regions where quasi-trapped electrons were originated.

satellite for time about 0.1 second. For relativistic electrons and positrons this flight time does not dependent from particle's rigidity. But if electron or positron has appropriate pitch-angle to be mirrored by magnetic field, flight time increases dramatically due to drift around the Earth. Drift speed is increasing with increasing of particle rigidity and so flight time of quasi-trapped particles is decreasing with rigidity as it is seen from figure. Such behavior of secondary albedo and quasi-trapped electrons and positrons correspond to that was observed in AMS-01 experiment [5] where they were called as short-lived and long-lived second leptons.

In figure 3,4 points of origin of reentrant electrons and positrons are shown., With agreement with previous observations by AMS-01 quasi-trapped electrons and positrons originated from specific regions (figure 5,6).

There is also a significant part of track with very large live-time which can not be determined by simple tracing procedure. Figure 7,8 shows calculated spatial position of trapped electrons and positrons they had 35 second before detection.

Figure 9 shows positron to electron ratio for different components. Results for quasi-trapped and short-lived albedo particles are consistent with measurements made in AMS-01 experiment [5] shown by open points in the figure. The ratio of positrons and electrons fluxes for stably trapped particles is much lower then for quasi-trapped particles. The maximum

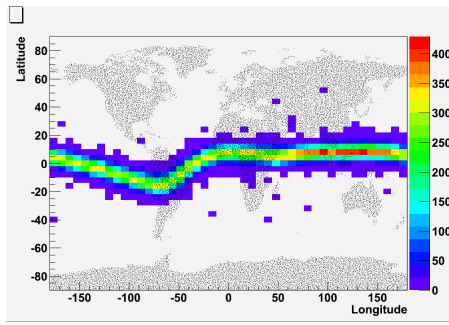


FIG. 7: Regions where trapped positrons were 35 second before detection.

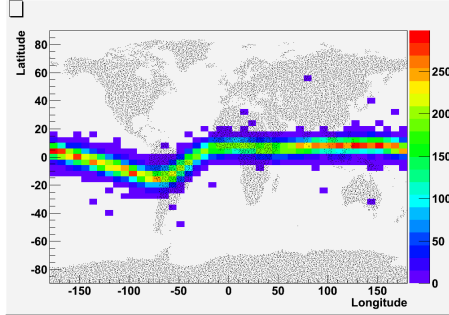


FIG. 8: Regions where trapped electrons were 35 second before detection.

counting rate of the trapped particles in the experiment observed on L-shell 1.18 and increases with decreasing in the value of the magnetic field. These results are difficult to explain in terms of the model of inelastic interaction of radiation belt protons with residual atmosphere [2], which predicts significant increase in positrons at least at low energies. Results of measurements suggest a more efficient capture of electrons due to different boundary conditions for electrons and positrons near SAA or different time of live of trapped positrons and electrons.

IV. SUMMARY

Secondary electron and positron fluxes have complex spatial structure caused by geomagnetic field,

production cross-section and atmospheric absorption of produced secondaries. Using backtracking procedure over 10^6 events three components of secondary positrons were clearly separated: albedo, quasi-trapped and stably trapped. Measured positron to electron ratio in the PAMELA experiment points out on different production mechanism of trapped and quasi-trapped particles.

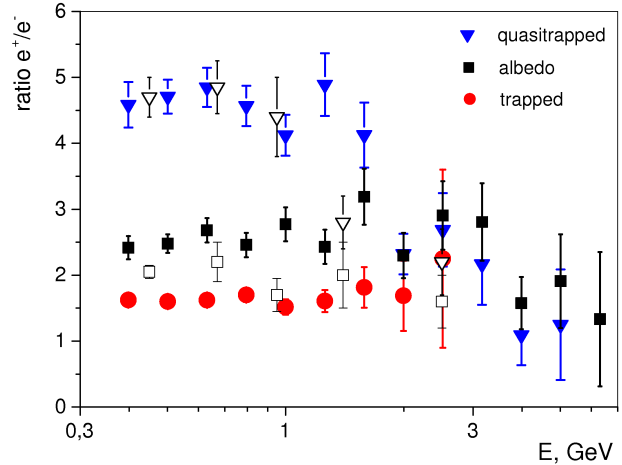


FIG. 9: e^+/e^- ratio vs energy for quasi-trapped, albedo and trapped components. AMS-01 data are shown by open points.

V. ACKNOWLEDGMENTS

We acknowledge support from Russian Federal Space Agency (Roscosmos), the Italian Space Agency (ASI), Deutsches Zentrum für Luft- und Raumfahrt (DLR), the Swedish National Space Board. V.V. M. would like to thank for the support from National Research Nuclear University MEPhI in the framework of the Russian Academic Excellence Project (contract No. 02.a03.21.0005, 27.08.2013).

- [1] N.L. Grigorov, Paper of AS USSR, 1977, **v. 24**, p. 810.
- [2] A.A. Gusev, U.B. Jayanthet, I.M. Martin et al., Journal of Geophys. Res. 2001,106,11,A26111.
- [3] O.Adriani et al.[PAMELA collaboration],Journal of Geophys. Res. 2009,A12218, doi:10.1029/2009JA014660.
- [4] V. Plyaskin, Astropart. Phys.,2008, **v.30**, p. 18.

- [5] Alcaraz, J., et al. Phys. Lett. B,2000,**v. 484**, p.10.
- [6] P. Picozza ,A.M. Galper, G. Castellini et al.[PAMELA collaboration],Astropart. Phys. 2007, **v.27**, p.296-315.
- [7] O.Adriani et al.[PAMELA collaboration],Phys.Rep. 2014, **v.544**, 4, p.323-370.